

**Hydrogenation of the dominant interstitial defect in irradiated boron-doped silicon**

N. Yarykin\* and O. V. Feklisova

*Institute of Microelectronics Technology RAS, Chernogolovka, Moscow region 142432, Russia*

J. Weber

*TU Dresden, 01062 Dresden, Germany*

(Received 8 May 2003; revised manuscript received 10 September 2003; published 9 January 2004)

The H3-center with a level at  $E_v + 0.535$  eV is observed in hydrogenated electron-irradiated boron-doped silicon. In samples with boron concentrations of  $(2-20) \times 10^{15} \text{ cm}^{-3}$  the center is the most abundant among all defects detected by deep-level transient spectroscopy. Electrical properties and thermal stability of the H3-center are studied in detail. It is shown that the H3-center is created by the addition of one hydrogen atom to a radiation-induced defect, the H3 precursor, which escapes direct electrical detection in the samples. The H3 precursor is formed immediately after room-temperature irradiation in oxygen-lean crystals and after heat treatment at  $\sim 200$  °C in oxygen-rich wafers. The H3 precursor anneals out at  $\sim 375$  °C in all samples. The introduction rates of H3 precursor and other radiation defects are measured for samples with different boron concentrations. The identification of H3 precursor as the  $B_iC_s$  pair and H3-center as a BCH complex is in good agreement with the available experimental data.

DOI: 10.1103/PhysRevB.69.045201

PACS number(s): 61.72.Ji, 61.82.Fk, 71.55.Cn

**I. INTRODUCTION**

Radiation defects and hydrogen atoms are introduced during many treatments of silicon crystals, and there is an urgent need to understand the interaction of these defects in detail. During the last two decades many studies were published in the field, and several defects have been identified by their electrical or optical activities as complexes of radiation defects with one or more hydrogen atoms. In the present paper we consider only complexes formed by a subsequent hydrogenation of stable defects which were created by room-temperature electron irradiation.<sup>1-8</sup>

Hydrogen was found to passivate the electrical activity of all defects introduced in silicon by irradiation with high-energy electrons.<sup>1</sup> Recently, this process was studied for major radiation defects in more detail. The VO center (a vacancy trapped by an interstitial oxygen atom, the A center) can bind one or two hydrogen atoms. The VOH center with energy levels at  $E_c - 0.31$  eV and  $E_v + 0.28$  eV ( $E_c$  and  $E_v$  are the bottom of conduction band and the top of valence band, respectively) was detected by deep-level transient spectroscopy (DLTS) (Refs. 3, 5, and 9) and by EPR.<sup>10</sup> The electrically passive VOH<sub>2</sub> complex was identified by IR absorption.<sup>6</sup> The major interstitial-type defect in oxygen-rich crystals, the  $C_iO_i$  pair, was shown to lose its electrical activity due to the addition of one hydrogen atom.<sup>7</sup> Very recently, the  $C_iO_iH$  complex has been identified with the D1-center, the unique bistable defect detected by Hall effect, IR absorption, and DLTS.<sup>8,11,12</sup> The  $C_iC_s$  pair, which is important in carbon-rich, oxygen-lean crystals, can also be passivated due to interaction with hydrogen atoms.<sup>7</sup>

An important class of radiation defects in silicon are those related to shallow level impurities, e.g. boron in *p*-type silicon crystals. The boron impurity in nonirradiated Si occupies substitutional positions ( $B_s$ ) and participates in the formation of radiation defects by trapping migrating intrinsic point defects, vacancies and self-interstitials. The  $B_sV$  complex is rather unstable and anneals out at 260–280 K.<sup>13</sup> Trapping

self-interstitials produces the interstitial boron species,  $B_i$ , which are mobile above  $\sim 240$  K (Ref. 14) and can be trapped by other defects. Several deep levels were reported in the literature to originate from such complexes.

A level at  $E_c - 0.26$  eV was ascribed to the  $B_iO_i$  pair because of the dependence of its concentration on the boron and oxygen contents.<sup>15,16</sup> The huge asymmetry of electron and hole capture cross sections to this level ( $\sigma_e = 2 \times 10^{-13} \text{ cm}^{-2}$ ,  $\sigma_p \sim 10^{-20} \text{ cm}^{-2}$ ) (Ref. 15) insures that the complex can be reliably detected in *p*-type samples using minority carrier transient spectroscopy (MCTS). Note that  $B_iO_i$  is abundant only in oxygen-rich Cz-Si, while its introduction rate is many times lower in oxygen-lean FZ-Si.<sup>17</sup>

The  $B_iO_i$  pair dissociates at 150–200 °C and the H(0.29) center with a level at  $E_v + 0.29$  eV appears in the same temperature range. Activation energies and frequency factors for the disappearance of the  $B_iO_i$  pairs and for growth of the H(0.29) centers are nearly the same.<sup>15</sup> Due to this correlation, the H(0.29) center was associated with an interstitial boron-related defect. Because capture of migrating  $B_i$  species at carbon impurity atoms was expected, the H(0.29)-center was tentatively identified as a  $B_iC_s$  pair.<sup>16</sup> We discuss this identification in Sec. III C 4 in more detail.

A donor level at  $E_v + 0.30$  eV [H(0.30)] (Ref. 38) was observed in as-irradiated crystals with higher boron doping.<sup>16</sup> The H(0.30)-center introduction rate increases as the square of the boron concentration, indicating that two boron atoms are involved in the center. Because of its obvious formation mechanism, the H(0.30) center was ascribed to a  $B_iB_s$  pair. However different calculations agree that the  $B_iB_s$  pair should be electrically inert.<sup>18-20</sup> Another candidate for the H(0.30) center seems to be a pair of substitutional boron atoms on neighboring sites.<sup>21</sup> The pair is expected to be electrically active,<sup>18</sup> although the complex stability is still uncertain.<sup>18,19</sup>

At present, the interaction of boron-related  $B_iO_i$ , H(0.29), and H(0.30) complexes with hydrogen is not known. Re-

cently, several groups reported on two deep-level centers in irradiated boron-doped silicon.<sup>4,22</sup> The centers labeled MH3 and H3 were shown to be hydrogen-related.<sup>23</sup> MH3 is created by the trapping of a migrating interstitial-type defect, most probably the  $B_i$  species, on the preformed  $B_sH$  pair forming a  $B_iB_sH$  complex. The nature of the hydrogen-related H3 center, which strongly dominates the deep-level spectrum of some boron-doped crystals,<sup>22</sup> is still unknown. In the present article, we investigate in detail the electrical properties, thermal stability, and formation kinetics of the H3 center. In addition we will demonstrate its boron-related origin and discuss the nature of its (nonhydrogenated) precursor.

## II. EXPERIMENT

### A. Samples

The samples used in this study were cut from boron-doped silicon wafers grown by either the float zone (FZ) or the Czochralski (Cz) method. Boron concentrations were varied in the range  $[B] = (0.4-20) \times 10^{15} \text{ cm}^{-3}$ . The nominally boron-free aluminum-doped wafers ( $[Al] = 1.3 \times 10^{16} \text{ cm}^{-3}$ ) were also used in a few cases. The samples were irradiated with 5.5 MeV electrons at a flux of  $\sim 10^{12} \text{ cm}^{-2} \text{ s}^{-1}$  to doses in the range  $D = (0.03-7) \times 10^{15} \text{ cm}^{-2}$ . The samples were either cooled during irradiation by air convection (temperature rise up to  $\sim 60^\circ \text{C}$ ), or placed on a water-cooled plate. Samples were annealed after irradiation in the temperature range from 100 to  $400^\circ \text{C}$  in a furnace under flow of inert gas.

Hydrogenation of irradiated samples was produced during wet chemical etching in an acid solution of  $\text{HF}:\text{HNO}_3:\text{CH}_3\text{COOH}$  (1:2:1) at ambient temperatures. The etching rate was about  $20 \mu\text{m}/\text{min}$ . After etching, most of the hydrogen atoms are trapped in the form of electrically inert boron-hydrogen ( $B_sH$ ) pairs located in a narrow near-surface layer, which is barely accessible with DLTS and CV techniques.<sup>24</sup> The  $B_sH$  pairs become unstable around  $100^\circ \text{C}$ .<sup>25</sup> Therefore the etched samples were annealed in a furnace at temperatures between 100 to  $200^\circ \text{C}$  to diffuse hydrogen deeper into the crystal and stimulate its interaction with radiation defects. Alternatively, the Schottky diodes prepared on the etched surface were annealed with a reverse bias applied (reverse-bias annealing, RBA) (Ref. 25) at 340 to 420 K.

### B. Capacitance measurements

Capacitance measurements were performed on Schottky diodes of 1, 1.5, or 2 mm diameter (depending on the doping level), which were fabricated by vacuum evaporation of Al at room-temperature. Ohmic contacts were produced by scratching the back side of the samples with an eutectic InGa alloy.

Most of the deep-level transient spectroscopy (DLTS) (Ref. 26) measurements were performed on a computerized system based on the modified Boonton 72B capacitance meter operated with the 1 MHz test signal. Different correlation functions were applied to the recorded capacitance

transients.<sup>27</sup> Durations of the transients were varied from 0.03 to 5 s. This system was operated in the temperature range 80 to 420 K. Another DLTS setup with the analog sine-wave lock-in correlation was equipped with a sample holder cooled down to 30 K and was used primarily for investigations of deep levels with peaks below 80 K. Activation energies and capture cross sections of the defects were determined from the Arrhenius plot of the emission rate using the standard  $T^2$ -correction. In addition, the capture cross section of some centers was measured by varying the filling pulse duration. The minority-carrier transient spectroscopy (MCTS) measurements were performed for semitransparent Schottky contacts using front-side photo-excitation from a light-emitting diode.

The spatial distributions of majority traps were calculated from the dependences of DLTS signal on the filling pulse voltage  $V_p$  at a fixed reverse bias  $V_r$ . The inhomogeneous profiles of shallow dopants, which were determined from the CV measurements, and the so-called transition region<sup>28</sup> (or  $\lambda$ -layer<sup>29</sup>) were properly included in the evaluation of the deep-level defect concentration. For the case of overlapping peaks, the interference of DLTS signals from different centers was also taken into account during profile calculations.

For presentation of the deep-level spectra throughout the paper, the measured DLTS signals were multiplied by a factor  $V_r/(V_r - V_p)$  to insure that defects with equal concentrations provide the peaks of approximately the same amplitude.

## III. RESULTS AND DISCUSSION

### A. Hydrogen-related levels

The effect of hydrogenation on the deep-level spectrum of electron-irradiated boron-doped FZ-Si is shown in Fig. 1. Hydrogen was introduced during chemical etching of irradiated crystal and redistributed deeper into the sample during subsequent 90 min annealing at  $100^\circ \text{C}$ . The significant decrease of the net boron concentration in the  $1.5 \mu\text{m}$  layer adjacent to the surface (see inset Fig. 1) indicates hydrogen penetration into this region. Therefore, the dashed line in Fig. 1 taken from the hydrogen-free region deeper than  $1.7 \mu\text{m}$  represents the spectrum of nonhydrogenated radiation defects. The spectrum is dominated by the donor level of the divacancy ( $V_2$ ) with a peak at 114 K. The peak of the  $C_iO_i$  center at 191 K is relatively low in the oxygen- and carbon-leak crystal. The nature of smaller peaks at  $\sim 225 \text{ K}$  and  $\sim 280 \text{ K}$ , which are observed after irradiation in most of the investigated FZ crystals, is unknown.

The solid line in Fig. 1 shows the deep-level spectrum of the hydrogenated region from 0.5 to  $1.5 \mu\text{m}$  depth. It is seen that the divacancy signal decreases in this region, and two new peaks appear at 139 K and 233 K. A level located at  $E_v + 0.28 \text{ eV}$  (corresponding to the peak at 139 K) was reported in virtually all publications on hole traps in hydrogenated irradiated silicon.<sup>2-4,30</sup> Recently this center has been identified as a donor level of the VOH complex (the singly hydrogenated A center).<sup>7</sup> The H3 peak at 233 K dominates the spectrum of the hydrogenated region of the sample in Fig. 1. Levels similar to H3 have been reported only in a few

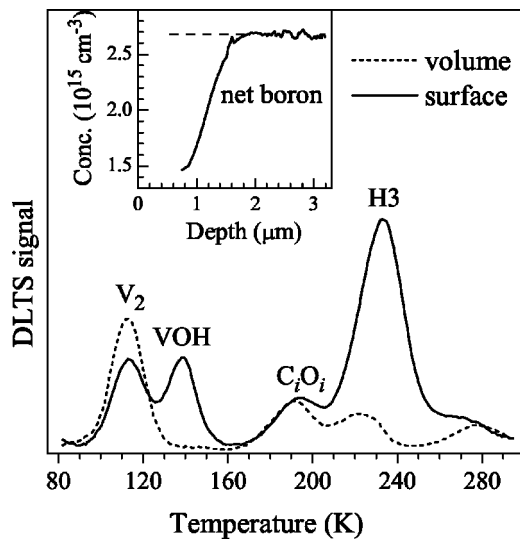


FIG. 1. DLTS spectra from the hydrogenated [surface ( $V_r/V_p = 3/0$  V), solid line] and nonhydrogenated [volume ( $V_r/V_p = 18/6$  V), dashed line] regions of irradiated FZ  $p$ -type Si ( $[B] = 2.7 \times 10^{15} \text{ cm}^{-3}$ ,  $D = 7 \times 10^{14} \text{ cm}^{-2}$ ). Hydrogenation by chemical etching was followed by 90 min annealing at 100 °C. Rate window  $49 \text{ s}^{-1}$ . The inset gives the net boron depth profile from CV measurements.

publications,<sup>4,22</sup> and the nature of the corresponding center is still unknown.<sup>39</sup> No deep-level centers are detected after a similar hydrogenation procedure of initial (non-irradiated) wafers, implying that the H3 center is a result of hydrogen interaction with a radiation defect. It is obvious from Fig. 1 that the concentration of the H3 center exceeds all other hole traps in the sample. Hence, no defect with a deep level in the lower half of the band gap can be a (non-hydrogenated) precursor of the H3 center. The nature and properties of the H3 center and its precursor will be of primary interest in this article.

## B. Properties of the H3-center

### 1. Electrical parameters

The activation energy of hole emission from the H3-center was determined by dependence of the DLTS peak position on the correlation function applied to the transient.<sup>26</sup> The period and the wave-form of correlation functions were varied to cover more than three orders of magnitude of the emission rate.<sup>27</sup> The Arrhenius plot obtained gives the activation energy of  $(0.535 \pm 0.005) \text{ eV}$  and the (apparent) capture cross section of  $1.7 \times 10^{-13} \text{ cm}^{-2}$ , which are in very good agreement with the parameters reported by Mamor *et al.*<sup>22</sup> The rather large value for the capture cross section could be a sign of a hole attractive center. In this case the hole emission rate is expected to depend on the electric field (Poole-Frenkel effect). The field dependence was studied by the double DLTS (DDLTS) technique on samples similar to those shown in Fig. 1. Emission from the H3-centers located in a layer between 0.5 to 1  $\mu\text{m}$  from the surface (see inset in Fig. 1) was measured under different reverse biases. The electric field in the investigated layer varied in the range

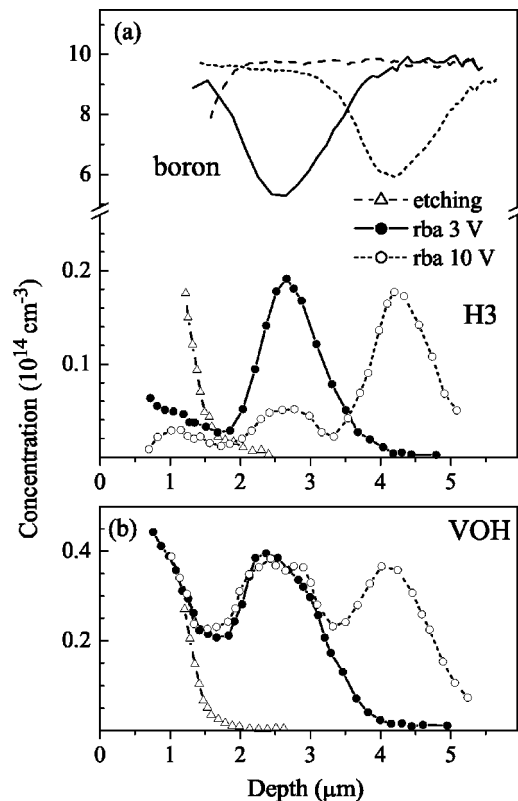


FIG. 2. Depth profiles of (a) the H3 centers and the net boron concentration and (b) the VOH centers in FZ-Si ( $D = 7 \times 10^{14} \text{ cm}^{-2}$ ). Samples were chemically etched and received two successive 90 min anneals at 380 K under reverse biases of 3 and 10 V, respectively.

$(2-8) \times 10^4 \text{ V/cm}$ . The shift of the H3 DDLTS peak is found to be less than the experimental error of 0.5 K, which is related to the reproducibility of the peak position during different thermal scans. At the same time, rough estimate based on the well-known expression for the Poole-Frenkel effect<sup>31</sup> gives a shift of more than 10 K in the studied range of electric fields. Thus, the H3 level belongs most probably to a donor.

The kinetics of hole capture on the H3 centers were studied directly by using the variation of filling pulse width. A noticeable decrease of the peak amplitude is observed only at the shortest available pulse (100 ns). A rough estimate of  $\sim 3 \times 10^{-15} \text{ cm}^{-2}$  can be obtained for the capture cross section from these measurements. This value is typical for capture at neutral centers and is in agreement with the donor nature of H3.

### 2. Thermal stability

The depth profiles of hydrogen-related centers formed by successive RBA treatments with increasing voltages are shown in Fig. 2 along with the net boron distributions calculated from the CV curves. During etching, most of hydrogen atoms are trapped at boron forming the electrically inert  $B_5H$  pairs in a near-surface layer. The H3 and VOH centers (with much lower concentrations than that of  $B_5H$ ) are also formed in this layer without any additional thermal treatment. To

redistribute hydrogen deeper into the crystal, the RBA procedure (annealing under reverse bias) (Ref. 25) was applied at 380 K. At this temperature the lifetime of  $B_sH$  pairs is only about 5 min. The released hydrogen atoms are positively charged and quickly drift away in the electric field of Schottky diode that suppresses the reverse reaction of  $B_sH$  formation. Thus, the near-surface region of the space charge region (SCR) gets virtually free of hydrogen in about 15 min. After this short treatment, most of hydrogen atoms form the  $B_sH$  pairs close to the SCR boundary, where the electric field turns to zero. Further redistribution takes place in the field-free region and is much slower. Note that because of the relatively short  $B_sH$  lifetime, a certain concentration of free hydrogen atoms (roughly proportional to the  $B_sH$  concentration) is maintained at 380 K, facilitating the complexing between hydrogen and radiation defects.

The first RBA step at 3 V (Fig. 2) moves hydrogen to around the  $2.6 \mu\text{m}$  depth, where the  $B_sH$ , H3, and VOH complexes are formed. During the second RBA step at 10 V, virtually all hydrogen atoms are rapidly moved to the deeper region around  $4.2 \mu\text{m}$  as monitored by the net boron depth profiles. Accordingly, additional H3- and VOH-centers are formed in this region. There is a different behavior for the H3 and VOH centers near  $1.2$  and  $42.6 \mu\text{m}$  during subsequent anneals. The A center concentration remains constant because no free hydrogen atoms were available in those regions to form additional centers or to transform VOH to the electrically inactive complex with two hydrogen atoms. In contrast, the H3-center concentration significantly decreases revealing an instability of the H3-centers in the space charge region of a Schottky diode at 380 K.

We rule out the possibility of a drift of the H3 center as a whole in the SCR electric field (at least at 380 K) due to the following two observations. First, the amount of the H3 centers in the deeper pile-up does not depend on the integral concentration of the centers formed during the first RBA step which can be controlled by the step duration. Second, the detailed studies of the H3 profile transformation during RBA at higher voltages reveal no drift of the preformed pile-up; in particular, the H3 center concentration remains always low at  $3.5 \mu\text{m}$  in Fig. 2(a). Therefore, we conclude that the H3 centers dissociate in SCR at 380 K.

The dissociation kinetics was investigated by dividing the annealing at higher voltage into shorter steps and measuring the decrease of the H3-center concentration in the region of preformed pile-up; e.g. the H3 decay at  $2.6 \mu\text{m}$  during RBA under the 10 V bias in Fig. 2(a). It is important to note that this is the hydrogen-free region after a short initial step as indicated by the nearly total recover of the net boron concentration. So, the process of H3-center dissociation is not masked by further defect formation or passivation. It is found that a part of the DLTS signal measured at the H3-peak maximum remains stable even after several hours of annealing. The nature of this signal is unknown, but its amplitude is only 5–15% of the initial signal in different samples. After subtraction of this stable part, the H3-center decay follows a simple exponential law (Fig. 3, solid symbols) with a characteristic time of about 1 h at 380 K. For the case of the lower doped sample (open symbols in Fig. 3), the

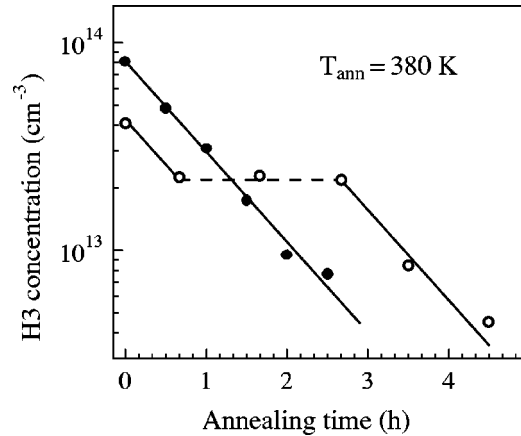


FIG. 3. Annealing kinetics at 380 K of the H3 center in the hydrogen-free region of *p*-type FZ-Si. Solid symbols:  $[B]=2.8 \times 10^{15} \text{ cm}^{-3}$ ,  $D=7 \times 10^{14} \text{ cm}^{-2}$ ; open symbols:  $[B]=8.7 \times 10^{14} \text{ cm}^{-3}$ ,  $D=10^{15} \text{ cm}^{-2}$ . Solid lines: annealing in the space charge region; dashed line: annealing in the neutral region.

reverse bias was switched off after a short initial RBA step, which removed hydrogen from the preformed pile-up region, and two 1-h-steps of zero-bias annealing were performed. It is seen that the H3 centers are stable under zero bias (in the neutral region) on the time scale of the experiment.

In general, different defect stabilities in the SCR and neutral region can be related either to different defect charge states or to the presence of the electric field in the SCR. To distinguish between these two possibilities we used the procedure of pulsed-bias annealing,<sup>32</sup> when the H3 centers inside the SCR are kept in the charge state inherent for neutral region ( $H3^{(+)}$  if H3 is a donor). The extrapolation of the Arrhenius curve for the hole emission from the H3 center (see Sec. III B 1) gives the emission time constant  $\sim 0.4 \mu\text{s}$  at 380 K. If the period of short filling pulses (zero bias) is comparable or smaller than this value, the H3 centers will be positively charged during a significant part of annealing time. In our experiments, the  $0.1 \mu\text{s}$  filling pulses were applied with a period of  $0.5 \mu\text{s}$ . Thus, the centers experienced the SCR electric field during 80% of annealing time. However, during only  $\sim 40\%$  of annealing time, the H3 centers were in the neutral charge state typical for steady state in SCR. The H3-center decay rate measured for the given conditions is 2.5 to 3 times lower than that measured without filling pulses. This result is in a good agreement with a model, which assumes that the H3-center thermal stability is primarily governed by its charge state. The stability of positively charged  $H3^{(+)}$  is much higher than the stability of the neutral center.

The temperature dependence of  $H3^{(0)}$ -center dissociation (the neutral charge state is realized in SCR) was studied in a set of identically prepared samples. A pile-up of the H3 centers was created in the near-surface region by 90 min furnace annealing at  $100^\circ\text{C}$  after chemical etching. Afterwards, Schottky diodes were evaporated and annealed under the pulsed-bias conditions at 380 K for 30 minutes. This treatment was sufficient to destroy all boron-hydrogen pairs and remove hydrogen from the near-surface region, but con-

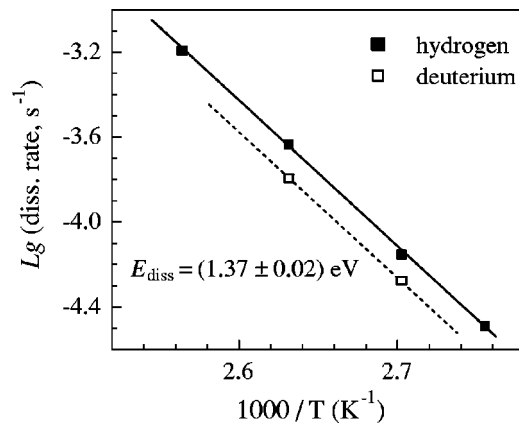


FIG. 4. Temperature dependence of the H3 center dissociation rate in the space charge region of a Schottky diode. Solid and open symbols correspond to hydrogenated and deuterated samples, respectively. The solid line is the best fit to the solid symbols. The dashed line is parallel to the solid one and shifted by  $\sqrt{2}$  along the ordinate axis.

served most of the preformed H3 centers. Finally, the diodes were annealed under reverse bias at different temperatures from 363 to 390 K. The decrease of H3 center concentration in the near-surface region with annealing time is exponential and the calculated dissociation rates are plotted in Fig. 4 with solid symbols. The best linear fit to the data gives a dissociation energy for the neutral H3 center of  $(1.37 \pm 0.02)$  eV and a pre-exponential factor of about  $2 \times 10^{14} \text{ s}^{-1}$ . A few samples were etched in an acid solution where 95% of hydrogen cations were replaced by deuterium. The H3 center concentration in deuterated samples was similar to that in hydrogenated ones. It is seen in Fig. 4 that dissociation of the H3<sup>(0)</sup>-centers in deuterated samples is slower by a factor of  $\sim \sqrt{2}$ , exactly as should be expected if the dissociating particle is hydrogen.

The positively charged H3 center is thermally stable at 380 K (see Fig. 3, open symbols). To study its stability at higher temperatures the etched samples (still without diodes) were annealed at temperatures from 380 to 450 K for 1 h. Since hydrogen was not removed from the investigated layer in this case, both formation and dissociation of the H3 centers took place during annealing. Therefore, the heat treatment was terminated by fast cooling to room temperature to avoid an additional formation of the centers at this stage. Finally, Schottky diodes were evaporated without any additional chemical treatment of the surface, and the H3 center depth profiles were measured. The maximum H3 center concentrations are  $\sim 2$  and  $\sim 5$  times lower after the anneals at 430 and 450 K, respectively, as compared to the concentration after 380 K treatment.

It is however not possible to determine quantitatively the properties of H3<sup>(+)</sup> centers from an analysis of these data. Due to a dynamic equilibrium between the two charge states of the H3 center in the neutral region, the center is neutral during a certain (small) fraction of time and subjected to the dissociation with (high) rate plotted in Fig. 4. Extrapolating the data from Fig. 4 to higher temperatures and accounting for the Fermi level position in the samples, one obtains for

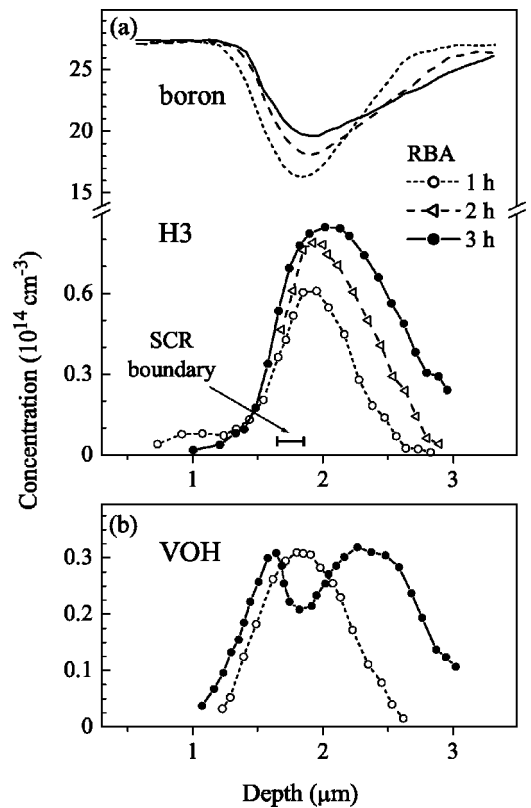


FIG. 5. Depth profiles of (a) the H3 centers and the net boron concentration and (b) the VOH centers in FZ-Si after three successive 1 h anneals at 380 K under reverse bias of 5 V ( $D = 7 \times 10^{14} \text{ cm}^{-2}$ ). The range for variation of the SCR boundary during annealing is indicated.

this dissociation mechanism the time constants of about 4 and 0.4 h at 430 and 450 K, respectively. This explains fairly well the observed decrease of the maximum concentration of H3 centers in corresponding samples. Thus, we conclude that the thermal stability of the H3<sup>(+)</sup> center is close to, or even higher than, the limit imposed by the dissociation rate of the neutral center.

### 3. Formation kinetics

The development of the deep-level depth profiles during the RBA procedure at 380 K is shown in Fig. 5. Depth distributions of the H3 and VOH centers after the first hydrogenation step are similar (dotted curves). At this stage, the process is governed by the addition of a single hydrogen atom to the respective precursors. For longer hydrogenation, the VOH profile exhibits a decrease in the region of maximum hydrogen concentration around  $1.9 \mu\text{m}$  in Fig. 5(b). This decrease is caused by the further hydrogenation of the VOH center and its transformation to the electrically passive VOH<sub>2</sub> complex.<sup>7,30</sup> No indications of such behavior have been found for the H3 centers for as long as 9 h hydrogenation at 380 K. In contrast, the H3 center concentration reveals a saturation in the region of maximum hydrogenation, although hydrogen is still available in this region as seen from the net boron concentration [see Fig. 5(a)]. This behavior is consistent with a model, which assumes only one hy-

drogen atom in the H3 center and a negligible binding of a second hydrogen at 380 K. A long hydrogenation time results in the consumption of nearly all H3 precursors. Under these conditions the H3 center concentration is a measure of the initial precursor concentration.

The H3 center formation during hydrogenation can be described by equation

$$[H3](\Phi) = [H3]_0 [1 - \exp(-r\Phi)], \quad (1)$$

where  $[H3]$  is the concentration of the H3 centers,  $[H3]_0$  the initial concentration of the H3 precursor,  $r$  the radius of hydrogen capture to the precursor, and  $\Phi$  the “hydrogenation dose.” The value  $\Phi$  is proportional to the free-hydrogen concentration  $[H]$  at a given point integrated over annealing time:

$$\Phi(t) = \int_0^t 4\pi D_H [H] dt, \quad (2)$$

where  $D_H$  is the hydrogen diffusivity.<sup>33</sup> The  $D_H[H]$  combination is found from the net boron concentration taking into account that equilibrium is reached in the reaction of boron–hydrogen pair formation/dissociation.<sup>25</sup> Eq. (1) is valid only if the hydrogen-related complex that is formed is thermally stable. Accounting for the dissociation of H3 centers in the space charge region at 380 K (Fig. 3), only data from the layer of 2.1–2.7  $\mu\text{m}$  [Fig. 5(a)] placed well inside the neutral region, are included in the calculations. A fit of the experimentally measured H3 center concentration as a function of calculated  $\Phi$  determines  $[H3]_0$  and  $r$ . For the sample shown in Fig. 5,  $[H3]_0 = 0.95 \times 10^{14} \text{ cm}^{-3}$ ; thus,  $\sim 90\%$  of precursors have been converted to the H3 centers. Averaging over different samples, we determine a capture radius of hydrogen to the H3 precursor of  $r = (0.65 \pm 0.15) \text{ nm}$  at 380 K. This value is not strongly dependent on temperature. Indeed, approximately the same maximum concentrations of H3 centers are detected immediately after chemical etching at room temperature and after long RBA steps at 380 K (Fig. 2).

### C. H3 precursor

The results presented above show that the H3 center is a complex of one hydrogen atom and an unknown radiation-induced defect, the H3 precursor. As H3 is the most abundant center in the hydrogenated region of irradiated FZ crystals (see Fig. 1), the H3 precursor is one of the dominant radiation defects in non-hydrogenated silicon. To learn more about the precursor, its introduction rate and behavior under annealing have been studied. We use the result from the previous section that the maximum H3 center concentration after a long enough hydrogenation at 380 K is almost equal to the precursor initial concentration.

#### 1. Formation and annealing temperature

The H3 centers are detected in all FZ Si crystals studied which were doped with boron in the range of  $(0.8\text{--}15) \times 10^{15} \text{ cm}^{-3}$ . Annealing of the irradiated samples at temperatures up to 300  $^\circ\text{C}$  has no effect on the concentration of

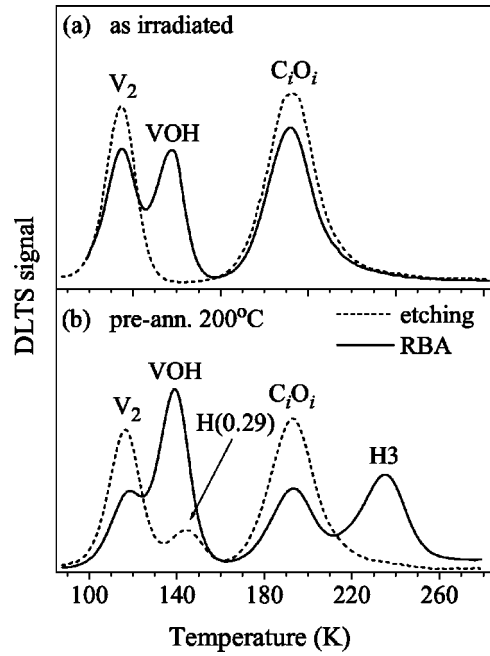


FIG. 6. The effect of hydrogenation on the DLTS spectrum of Cz-grown  $p$ -type crystal (a) irradiated at room temperature and (b) annealed after irradiation at 200  $^\circ\text{C}$  for 30 min. The dashed and solid curves were taken before and after hydrogenation, respectively. Hydrogenation by chemical etching and subsequent RBA (2 V) at 380 K during 100 min.  $[B] = 2.6 \times 10^{15} \text{ cm}^{-3}$ ,  $D = 3 \times 10^{15} \text{ cm}^{-2}$ .  $V_r/V_p = 4/1 \text{ V}$  and rate window is  $49 \text{ s}^{-1}$  for all spectra.

the H3 centers formed during further hydrogenation. Thus, we conclude that formation of the H3 precursor in FZ crystals is already completed during (or shortly after) irradiation at room temperature. An increase of the annealing budget up to 350  $^\circ\text{C}$  for 30 min, results in a significant decrease (from 2 to 5 times in different crystals) of the H3 precursor concentration. Finally, the H3 centers are not found in the samples, which were annealed at 375  $^\circ\text{C}$  for 30 min after irradiation.

Existence of the H3 centers was not reported in the previous studies performed on Cz-grown irradiated crystals.<sup>3,30</sup> In the present study, we confirm the absence of H3 centers in such crystals. Five different Cz crystals with boron doping in the range of  $(0.4\text{--}20) \times 10^{15} \text{ cm}^{-3}$  were irradiated at room temperature and then hydrogenated by chemical etching followed by prolonged RBA treatment at 380 K. No H3 centers are detected in these samples [see Fig. 6(a)]. At the same time, the VOH-level is found in all crystals indicating the presence of hydrogen in the investigated regions.

However, if the irradiated Cz-Si crystals were annealed at 200  $^\circ\text{C}$  for 30 min, subsequent hydrogenation forms the H3 peak as shown in Fig. 6(b). The electrical parameters of the center, the formation kinetics during hydrogenation, and the thermal stability (including the strong dependence on charge state) are identical to those for the H3 center in FZ crystals. Thus, the H3 precursor is formed in oxygen-rich Cz crystals upon post-irradiation annealing at 200  $^\circ\text{C}$ . As in the FZ crystals, an increase of the annealing temperature up to (350–375)  $^\circ\text{C}$  also destroys the H3 precursor in Cz samples.

In accordance with previous studies,<sup>15,16</sup> the H(0.29) center appears both in FZ- and Cz-Si at approximately the same annealing temperature as the H3 precursor in Cz-Si [see, e.g., Fig. 6(b)]. However, the H3 precursor concentration exceeds that of H(0.29) centers in all studied crystals with boron doping above  $\sim 10^{15} \text{ cm}^{-3}$ .

## 2. Electrical activity

As seen in Fig. 6 the annealing at 200 °C, which forms the H3 precursor, is accompanied by a rather minor transformation of the hole trap spectrum in non-hydrogenated samples. This indicates again that the observed hole traps cannot be associated with the H3 precursor. If the H3 precursor introduces any levels in the band gap, they are either shallower than  $\sim 0.1 \text{ eV}$  from the valence band or in the upper half of band gap. The latter possibility was checked by MCTS measurements from 77 to 300 K. None of the minority carrier traps observed by MCTS exhibit the thermal stability similar to that of the H3 precursor as determined in previous section. However, due to the low photoexcitation level, only the traps with electron capture cross sections above  $\sim 5 \times 10^{-15} \text{ cm}^{-2}$  are expected to contribute to our MCTS signal. Thus, the question about electrical activity of the H3 precursor remains open. Note that the hydrogen capture radius of 0.5–0.8 nm found in section III B 3 for H3-center formation in the neutral region of *p*-type silicon, suggests the binding of a positively charged hydrogen atom with a neutral rather than a negative complex.

## 3. Introduction rate

Our measurements show that the H3 precursor concentration as well as the concentrations of other most prominent radiation defects in our samples are proportional to the irradiation dose. Hence, the introduction rate (the ratio of defect concentration to irradiation dose) can be calculated. The H3 precursor concentration in FZ-Si was taken equal to the maximum concentration of H3 centers after a long enough hydrogenation of as-irradiated samples. For the case of Cz-wafers, the post-irradiation annealing at 200 °C was used before hydrogenation to form the maximum concentration of H3 precursor. The results for different crystals (Cz and FZ) are presented with solid symbols in Fig. 7. The H3 precursor introduction rate exhibits a near linear increase with doping at low boron concentrations and a saturation when the boron concentration exceeds  $\sim 3 \times 10^{15} \text{ cm}^{-3}$ . Usually, such dependence is interpreted as involvement of one boron atom in the investigated complex.<sup>40</sup>

The total introduction rate of H3 centers and all known interstitial-type complexes detected in the samples, is shown in Fig. 7 with open symbols. The interstitial-type defects in our samples are mainly the  $C_iO_i$  and  $C_iC_s$  pairs. The H(0.30) centers also contribute to the sum in FZ samples with higher doping.<sup>41</sup> The dash-dotted line, which is the best linear fit to the open symbols, shows that such a sum is almost independent of the doping level. A similar slight decrease with the increase of boron concentration is found for the divacancy introduction rate (dashed line in Fig. 7). This behavior leads us to the conclusion that the H3 precursor is of interstitial

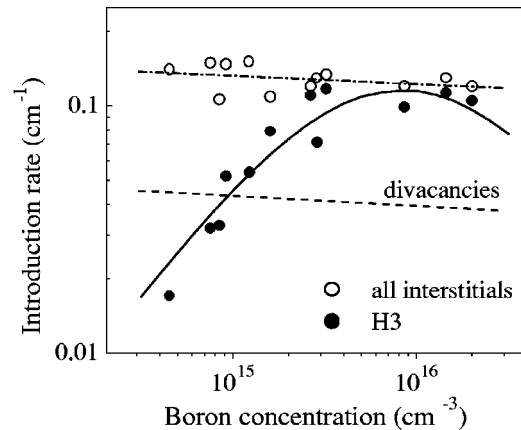


FIG. 7. Introduction rate of the H3 centers (solid symbols) and the sum of introduction rates for the H3 centers and all interstitial-type complexes (open symbols) in samples with different boron concentrations. The dashed line shows the divacancy introduction rate.

nature and dominates the spectrum of interstitial-type radiation defects in the  $(2-20) \times 10^{15} \text{ cm}^{-3}$  range of boron concentration. In addition, the interstitial nature of the H3 precursor is supported by the strong (up to 2 times) increase of  $C_iO_i$  pair concentration in Cz samples due to the heat treatment around 350 °C, which destroys the H3 precursor.

## 4. Discussion on the nature of the H3 precursor

The most important reactions of interstitial defects in silicon were considered by Zhao *et al.*,<sup>34</sup> and the introduction rates of stable complexes were calculated as functions of impurity content. Among boron-related defects, only the  $B_iO_i$  and  $B_iC_s$  pairs show a linear increase with boron concentration and a subsequent decrease due to competition with the  $B_iB_s$  complexes. Actually, such behavior is expected for any complex formed by  $B_i$  trapping to a background impurity with a high enough concentration. However, taking into account that the H3 centers have been observed in all crystals studied, we expect this trap to be a common impurity in silicon. Obviously, the H3 precursor cannot be identified as  $B_iO_i$  due to the missing correlation with oxygen content and a quite different thermal stability. Therefore, we propose the  $B_iC_s$  pair as the H3 precursor.

The solid curve in Fig. 7 has been calculated by the formula

$$[B_iC_s] = [Si_i] \frac{r_B[B]}{(r_B[B] + r_C[C])} \frac{r_{BC}[C]}{(r_{BC}[C] + r_{BB}[B])}, \quad (3)$$

where  $r$  with subscript B, C, BC, or BB are the effective capture radii for formation of the  $B_i$ ,  $C_i$ ,  $B_iC_s$ , and  $B_iB_s$  defects, respectively, brackets denote the concentration values. The first term  $[Si_i]$  is the concentration of silicon self-interstitials, which escapes recombination with vacancies. The second term describes the  $B_i$  formation by dividing the self-interstitials between the  $B_s$  and  $C_s$  traps. The final term stands for the  $B_iC_s$  formation with the competition for  $B_i$

from the  $B_iB_s$  pairs. Data on the capture radii are rather scattered in literature. It was cited in Ref. 35 that the interaction of mobile self- and boron interstitials with negatively charged substitutional boron is several times stronger than with neutral impurities. On the other hand, equal radii were used for the  $B_i$  and  $C_i$  formation in the later work.<sup>34</sup> Therefore, the approximation  $r_C/r_B=r_{BC}/r_{BB}=\alpha$  is accepted below. In this case, only two independent parameters exist in Eq. (3), the product  $\alpha[C]$  and the scaling factor  $[Si_i]$ . The value of  $\alpha[C]=8\times 10^{15}\text{ cm}^{-3}$  provides the best fit to the experimental points in Fig. 7 (solid curve). Taking into account that carbon concentration in the investigated crystals may vary, the fit is reasonably good.

Generally, the alternative mechanism to create the  $B_iC_s$  pair, the capture of migrating  $C_i$  species to  $B_s$ , is also possible in FZ crystals. In Cz-Si, most of the  $C_i$  species form  $C_iO_i$  pairs, which are stable under 200 °C annealing. The same (within the scatter of points in Fig. 7) amount of the H3 centers formed in Cz and FZ crystals shows that the alternative mechanism is less effective.

As mentioned in Sec. I, another defect, the H(0.29) center, was tentatively identified in the literature as the  $B_iC_s$  pair due to its formation kinetics which are correlated with the dissociation of the  $B_iO_i$  pairs. The main problem with this identification is that the H(0.29) centers are not detected in as-irradiated samples, even in oxygen-lean FZ-Si (Ref. 17) where the concentration of the competing  $B_iO_i$  pairs is negligible. In the FZ samples used in the present work, the concentration of the H(0.29) centers formed due to the 200 °C annealing exceeds more than 10 times the initial concentration of the  $B_iO_i$  pairs. Along with the unexpected introduction rate for  $B_iC_s$ ,<sup>17</sup> this indicates probably the more complicated nature of the H(0.29) center.

On the other hand, the identification of the H3 precursor as a  $B_iC_s$  pair agrees well with all experimental findings. Indeed, the pair is formed immediately during irradiation of oxygen-lean FZ crystals due to the capture of mobile  $B_i$  species by substitutional carbon atoms. In oxygen-rich Cz-crystals, all  $B_i$  species are first trapped by oxygen, and no H3 centers are detected in as-irradiated Cz samples. Upon annealing of the  $B_iO_i$  pairs around 200 °C, the situation for  $B_i$  becomes similar to that in FZ crystals, and the H3 centers can be formed with a similar concentration. Comparison of the DLTS and MCTS data shows that the H3 precursor concentration in the sample presented in Fig. 6(b) is at least half of the  $B_iO_i$  concentration in the same sample before annealing.

The assignment of the H3 precursor to the  $B_iC_s$  pair is in good agreement with recent calculations.<sup>20,36</sup> Both works

predict the dissociation of the pair by  $C_i$  emission that is experimentally supported by the increase of  $C_iO_i$  pair concentration upon annealing of the H3 precursor. The calculated binding energy of (1.1–1.2) eV corresponds fairly well to the annealing of the H3 precursor around 375 °C. Finally, the absence of the H3 precursor energy levels in the range accessible by DLTS in  $p$ -type silicon, correlates with results by Liu *et al.*,<sup>36</sup> which assume that the  $B_iC_s$  pair has only an acceptor level in the upper half of the band gap.

#### IV. CONCLUSION

The H3 level ( $E_v+0.535$  eV) is formed due to hydrogenation of electron irradiated boron-doped silicon. Based on the absence of Poole-Frenkel effect, the level is attributed to the  $H3^{(+/0)}$  transition. The thermal stability of the center is shown to depend strongly on the charge state. The neutral  $H3^{(0)}$  center is dissociated by hydrogen release with an activation energy of 1.37 eV. The stability of the positively charged  $H3^{(+)}$  center is higher and is most probably governed by hole emission and subsequent decay of the neutral complex. It is concluded from the complex formation kinetics during hydrogenation that the H3 center is created by capture of one hydrogen atom at a neutral (in  $p$ -type) radiation defect, the H3 precursor.

The H3 precursor formation is completed during room-temperature irradiation of oxygen-lean FZ crystals. An additional 30 min annealing at 200 °C is required to form the defect in Cz samples. The H3 precursor is destroyed by 30 min anneal at 375 °C both in FZ and Cz irradiated wafers. The introduction rate of the H3 precursor increases linearly with boron concentration in the range  $[B]=(0.4-3)\times 10^{15}\text{ cm}^{-3}$  and saturates in the range  $[B]=(3-20)\times 10^{15}\text{ cm}^{-3}$ . In the samples with  $[B]\geq 2\times 10^{15}\text{ cm}^{-3}$ , the H3 precursor is the most abundant interstitial-type complex.

Analysis of the interstitial defect reactions suggests that the  $B_iC_s$  pair is the most suited candidate for the H3 precursor. This assignment is in agreement with all present experimental results.

#### ACKNOWLEDGMENTS

We would like to thank R. Jones for sending us preprints of his works and for helpful discussions. Fruitful discussions with E. Yakimov are greatly appreciated. The expert technical assistance of B. Köhler and N. Tkacheva are acknowledged. The work was supported by Deutsche Forschungsgemeinschaft (436 RUS 113/166/0) and Russian Foundation for Basic Research (RFBR-DFG 00-02-04002).

\*Electronic address: nay@ipmt-hpm.ac.ru

<sup>1</sup>S. J. Pearton, Phys. Status Solidi A **72**, K73 (1982).

<sup>2</sup>K. Irmscher, H. Klose, and K. Maass, J. Phys. C **17**, 6317 (1984).

<sup>3</sup>O. V. Feklisova and N. Yarykin, Semicond. Sci. Technol. **12**, 742 (1997).

<sup>4</sup>S. Fatima, C. Jagadish, J. Lalita, B. G. Svensson, and A. Hallén, J. Appl. Phys. **85**, 2562 (1999).

<sup>5</sup>Y. Tokuda, H. Shimada, and A. Ito, J. Appl. Phys. **86**, 5630 (1999).

<sup>6</sup>V. P. Markevich, L. I. Murin, M. Suezawa, J. L. Lindström, J. Coutinho, R. Jones, P. R. Briddon, and S. Öberg, Phys. Rev. B **61**, 12964 (2000).

<sup>7</sup>O. V. Feklisova, E. B. Yakimov, N. Yarykin, and J. Weber, Semiconductors **35**, 1355 (2001).



- <sup>8</sup>J. Coutinho, R. Jones, P. R. Briddon, S. Öberg, L. I. Murin, V. P. Markevich, and J. L. Lindström, *Phys. Rev. B* **65**, 014109 (2002).
- <sup>9</sup>O. V. Feklisova, N. Yarykin, E. B. Yakimov, and J. Weber, *Physica B* **308–310**, 210 (2001).
- <sup>10</sup>P. Johannesen, B. Bech Nielsen, and J. R. Byberg, *Phys. Rev. B* **61**, 4659 (2000).
- <sup>11</sup>V. P. Markevich, M. Suezawa, K. Sumino, and L. I. Murin, *J. Appl. Phys.* **76**, 7347 (1994).
- <sup>12</sup>N. Yarykin and J. Weber, *Physica B* (to be published).
- <sup>13</sup>G. D. Watkins, *Phys. Rev. B* **13**, 2511 (1976).
- <sup>14</sup>J. R. Troxell and G. D. Watkins, *Phys. Rev. B* **22**, 921 (1980).
- <sup>15</sup>P. M. Mooney, L. J. Cheng, M. Sli, J. D. Gerson, and J. W. Corbett, *Phys. Rev. B* **15**, 3836 (1977).
- <sup>16</sup>P. J. Drevinsky, C. E. Cafer, S. P. Tobin, J. C. Mikkelsen, and L. C. Kimerling, *Mater. Res. Soc. Symp. Proc.* **104**, 167 (1988).
- <sup>17</sup>P. J. Drevinsky, C. E. Cafer, L. C. Kimerling, and J.L. Benton, in *Defect Control in Semiconductors*, edited by K. Sumino (Elsevier Science Publishers B. V., North-Holland, 1989), p. 341.
- <sup>18</sup>J. Zhu, T. Diaz de la Rubia, L. H. Yang, C. Mailhot, and G. H. Gilmer, *Phys. Rev. B* **54**, 4741 (1996).
- <sup>19</sup>X.-Y. Liu, W. Windl, and M. P. Masquelier, *Appl. Phys. Lett.* **77**, 2018 (2000).
- <sup>20</sup>J. Adey, R. Jones, and P. R. Briddon, *Appl. Phys. Lett.* **83**, 665 (2003).
- <sup>21</sup>A. K. Tipping and R. C. Newman, *Semicond. Sci. Technol.* **2**, 389 (1987).
- <sup>22</sup>M. Mamor, F. D. Auret, S. A. Goodman, W. E. Meyer, and G. Myburg, *Appl. Phys. Lett.* **72**, 3178 (1998).
- <sup>23</sup>N. Yarykin, O. V. Feklisova, and J. Weber, *Physica B* **308–310**, 159 (2001).
- <sup>24</sup>O. V. Feklisova, E. B. Yakimov, and N. Yarykin, *Semiconductors* **36**, 282 (2002).
- <sup>25</sup>T. Zundel and J. Weber, *Phys. Rev. B* **39**, 13549 (1989).
- <sup>26</sup>D. V. Lang, *J. Appl. Phys.* **45**, 3023 (1974).
- <sup>27</sup>S. Weiss and R. Kassing, *Solid-State Electron.* **31**, 1733 (1988).
- <sup>28</sup>L. C. Kimerling, *J. Appl. Phys.* **45**, 1839 (1974).
- <sup>29</sup>D. Stievenard and D. Vuillaume, *J. Appl. Phys.* **60**, 973 (1986).
- <sup>30</sup>O. V. Feklisova, N. Yarykin, E. B. Yakimov, and J. Weber, *Physica B* **273–274**, 235 (1999).
- <sup>31</sup>J. C. Bourgoin and M. Lannoo, *Point Defects in Semiconductors—Experimental Aspects* (Springer-Verlag, Berlin, 1983).
- <sup>32</sup>S. V. Koveshnikov, B. Choi, N. Yarykin, and G. A. Rozgonyi, *Physica B* **273–274**, 395 (1999).
- <sup>33</sup>N. Yarykin, J.-U. Sachse, H. Lemke, and J. Weber, *Phys. Rev. B* **59**, 5551 (1999).
- <sup>34</sup>S. Zhao, A. M. Agarval, J. L. Benton, G. H. Gilmer, and L. Kimerling, *Mater. Res. Soc. Symp. Proc.* **442**, 231 (1997).
- <sup>35</sup>L. C. Kimerling, M. T. Asom, J. L. Benton, P. J. Drevinsky, and C. E. Cafer, *Mater. Sci. Forum* **38–41**, 141 (1989).
- <sup>36</sup>C.-L. Liu, W. Windl, L. Borucki, S. Lu, and X.-Y. Liu, *Appl. Phys. Lett.* **80**, 52 (2002).
- <sup>37</sup>M. O. Aboelfotoh and B. G. Svensson, *Phys. Rev. B* **52**, 2522 (1995).
- <sup>38</sup>In spite of the very close activation energies, the H(0.29) and H(0.30) centers are resolved by standard DLTS rather well. The H(0.30) level gives a peak, which almost coincides with the signature of VOH complex, while the H(0.29) peak is located at  $\sim 10$  K higher temperature (see Fig. 6).
- <sup>39</sup>The H3 center could be confused with the H(0.52) center reported by Aboelfotoh *et al.*<sup>37</sup> in Cu-contaminated silicon with radiation defects. However, the DLTS signatures of the centers are slightly different. In addition, the H(0.52) center is formed in as-irradiated Cz-grown crystals that also distinguishes it from H3.
- <sup>40</sup>Generally, dependence on the doping level could be related with variation of the Fermi-level position. To check this possibility the Al-doped sample ( $[Al]=1.3\times 10^{16}$  cm<sup>-3</sup>, nominally boron-free) was irradiated and hydrogenated. No H3 centers are detected in this sample, although presence of the VOH complex indicates the successful hydrogenation.
- <sup>41</sup>Although the H(0.30)-center structure is uncertain, here and below we consider the complex as B<sub>i</sub>B<sub>s</sub> pair, because the B<sub>i</sub> species are believed to be necessary for the H(0.30)-center formation.